Journal of Inclusion Phenomena and Molecular Recognition in Chemistry **8**: 45–58, 1990.

Heat Capacity and Glass Transition of Ethylene Oxide Clathrate Hydrate*

O. YAMAMURO[1], Y. P. HANDA[2], M. OGUNI**, and H. SUGA‡
[1]*Department of Chemistry and Chemical Thermodynamics Laboratory, Faculty of Science, Osaka University, Toyonaka, Osaka 560, Japan*
[2]*Division of Chemistry, National Research Council of Canada, Ottawa, Ontario, Canada K1A OR9*

(Received: 28 March 1988; in final form: 4 May 1988)

Abstract. The heat capacity of structure I ethylene oxide clathrate hydrate EO·6.86 H_2O was measured in the temperature range 6–300 K with an adiabatic calorimeter. The temperature and enthalpy of congruent melting were determined to be (284.11 ± 0.02) K and 48.26 kJ mol^{-1}, respectively. A glass transition related to the proton configurational mode in the hydrogen-bonded host was observed around 90 K. This glass transition was similar to the one observed previously for the structure II tetrahydrofuran hydrate but showed a wider distribution of relaxation times. The anomalous heat capacity and activation enthalpy associated with the glass transition were almost the same as those for THF-hydrate.

Key words. Heat capacity, glass transition, clathrate hydrate, ethylene oxide hydrate.

1. Introduction

The three dimensional hydrogen-bonded network of water molecules in clathrate hydrates is similar to the one found in all the known forms of ice. However, the hydrogen bond in structures I and II hydrates resembles that in ice I_h more closely than in other ices in the sense that the average departure of the O—O—O bond angle in the hydrates is less than about 4% from the tetrahedral values found in ice I_h and the average O—O bond length in hydrates is only about 1% longer than in ice I_h. The infrared [1–3] and Raman [4] spectra, phonon density of states [5], and the electrical properties of the host lattice [6] of the hydrates are found to be similar to those of hexagonal ice, thereby indicating that the short-range order in the hydrate lattice and I_h are very similar.

The protons in hydrogen-bonded systems such as the ices I_h, I_c, V, and VI are configurationally disordered. If the temperature is sufficiently low, the protons get frozen-in in their disordered state and this gives rise to the well-known residual entropy observed in ice I_h crystals at 0 K. On warming such a system, an order-disorder transition related to the activation of the proton motion would be expected. For a long time such a transition was not observed in ice I_h, primarily due to the rather long relaxation time of the protons at low temperatures. However,

Issued as NRCC No. 30427. Contribution No. 140 from the Chemical Thermodynamics Laboratory.
* Dedicated to Dr D. W. Davidson in honor of his great contributions to the sciences of inclusion phenomena.
** Present address: Department of Chemistry, Faculty of Science, Tokyo Institute of Technology, O-okayama, Meguro-ku, Tokyo 152.
‡ Author for correspondence.

careful measurements in an adiabatic calorimeter on rapidly cooled and annealed samples of ice I_h revealed the presence of a small thermal anomaly around 100 K [7]. This anomaly was ascribed to the frozen-in configurational state of the protons and has been labelled as the glass transition. The situation in ice I_c is similar to that in I_h and a glass transition in ice I_c has recently been reported [8]. In ices V and VI, the relaxation time of the protons is much shorter and the order-disorder transition is easily observed [9]. Recently it was found [10] that by doping the crystal with a small amount (mole fraction $\sim 10^{-4}$) of an impurity such as KOH, the relaxation time can be lowered dramatically. Consequently, a first-order phase transition in KOH-doped crystals of ice I_h has been observed around 72 K where almost two-thirds of the configurational entropy is removed [11].

The similarity of the three-dimensional network of hydrogen bonded water molecules in hydrates and in ice I_h implies that the glass transition and the first-order transition observed in ice I_h should also be observed in hydrates. This was indeed found to be the case for the structure II tetrahydrofuran (THF) hydrate where careful heat capacity measurements showed a glass transition around 85 K [12] and a first-order phase transition around 62 K [13]. However, similar measurements on structure II argon hydrate did not show any anomaly in the pure sample but the KOH-doped sample showed a glass transition around 55 K [14]. Obviously the *nature* of the guest molecule affects both the relaxation time and the ordering of the protons.

In order to explore further the effect of the nature of the guest molecule on the characteristics of the glass transition, we have measured the heat capacity of ethylene oxide (EO) hydrate in the range 6–300 K with an adiabatic calorimeter. Ethylene oxide forms a typical structure I hydrate and has been studied quite extensively. The reorientational motion of the host and of the guest molecules in EO-hydrate has been investigated by structural [15, 16], dielectric [17, 18], NMR [18], and IR absorption [1, 19] studies. A glass transition, as observed in THF hydrate, is expected to occur around 100 K from the dielectric relaxation time data [18]. The heat capacity measurements by scanning calorimetry [20, 21] above 120 K did not reveal any thermal anomaly and there clearly is a need for precise heat capacity measurements especially at low temperatures.

2. Experimental

The calorimeter cell [12] and the adiabatic calorimeter [22] are described elsewhere. Ethylene oxide with a specified purity of 99.8 mol% was purchased from Fluka Chemie Agent and was used as such. Water used was distilled and deionized. Ethylene oxide (4.1015 g; 0.093103 mol) was degassed and charged by vacuum distillation into the calorimeter cell containing degassed water (11.5091 g; 0.63886 mol). Thus, the stoichiometric composition of the solution was EO·6.86 H_2O. Ethylene oxide forms a structure I hydrate of variable composition [23, 24] with EO·6.86 H_2O as the composition of the congruently melting hydrate [24] and thus our starting material contained a slight excess of EO relative to the ideal composition. The internal volume of the cell was 20.87 cm^3 and so the dead space inside the cell was about 5.2 cm^3. About 2×10^{-4} mol of helium gas were introduced in the cell to facilitate thermal contact between the sample and the cell.

The hydrate was prepared by slowly cooling the aqueous solution (0.06 K min^{-1}) from room temperature to 275 K where crystals first started to appear. It took about 70 min to complete the crystallization. The sample was subsequently annealed for 2 h at 283.2 K, just below its melting temperature of 284.2 K [24], and then cooled down to 120 K at the rate of 0.5 K min^{-1}. Further thermal history of the sample is given in the next section. Heat capacity measurements were carried out in the range 6–300 K. The precision of the measurements was ±1% around the lowest temperature and within ±0.1% above 30 K.

At the end of the calorimetric measurements, samples of EO and the aqueous solution used were transferred under vacuum to glass ampoules and stored for about six months before they were analyzed using a Perkin Elmer 3920 gas chromatograph. While EO was found to contain no detectable impurities, the aqueous solution was found to contain no EO but water (68 mol%), ethylene glycol (27 mol%), and diethylene glycol (5 mol%) only. The glycols presumably were produced by reaction of EO with water.

3. Results and Discussion

3.1. HEAT CAPACITY OF EO·6.86 H_2O

Below 120 K, two series of heat capacity measurements were performed. In one series the sample was cooled rapidly (1.1 K min^{-1}) from 120 K to ~50 K and in the other series the sample was annealed at 76.6 K for 24 h. These two measurements gave different results, indicating a time dependent nature of the heat capacity. Such a phenomenon is usually associated with a glass transition, as found previously [7, 8, 12, 14].

The experimental results of the heat capacity of the *rapidly cooled* and the *annealed* samples are collected in Table I as the quantities per mol of EO·6.86 H_2O. For the annealed sample, only the data between 60 and 120 K are reported because the heat capacities below 60 K were the same for both the annealed and the rapidly cooled samples.

At high temperatures, especially in the liquid state of the specimen, the experimental heat capacity is not precisely C_p but contains a contribution from vaporization of the sample. This is caused by the fact that the vapor pressure of the aqueous solution [25] is only slightly lower than the rather high vapor pressure of pure EO [26], (the normal boiling temperature of EO is 284 K), and there is considerable dead space (5.2 cm^3) inside the cell. The contribution was estimated to be 0.2 J K^{-1} (about 0.4% of sample heat capacity) based on vapor pressure data of EO [26] and thus represents the maximum contribution.

Figure 1 shows the heat capacity results of the rapidly cooled sample. There are five anomalies in the heat capacity curve. The most interesting one is the heat capacity jump at 90 K. This is due to the glass transition initially expected and is described in a separate section below. The largest anomaly at 284 K is due to the congruent melting of the hydrate and its details are also given below. Besides the above two, three unexpected and unwelcome anomalies appeared. The smallest of the three around 160 K is most likely the eutectic melting of excess EO and EO-hydrate because its temperature is slightly lower than the melting temperature of pure EO (160.65 ± 0.05) K reported by Giauque and Gordon [26].

Table I. Molar heat capacities of EO·6.86 H_2O

T_{av}/K	$C_{p,m}$/J K^{-1} mol^{-1}	T_{av}/K	$C_{p,m}$/J K^{-1} mol^{-1}	T_{av}/K	$C_{p,m}$/J K^{-1} mol^{-1}	T_{av}/K	$C_{p,m}$/J K^{-1} mol^{-1}
		79.74	143.1	181.44	232.4	283.68	15610
rapidly cooled		80.99	144.9	183.19	234.0	283.73	17860
6.64	1.945	82.24	146.7	184.94	235.6	283.77	20560
7.35	2.675	83.49	148.6	186.70	237.1	283.80	23740
8.19	3.663	84.73	150.5	188.47	238.7	283.84	27700
8.97	4.634	85.98	152.3	190.23	240.4	283.86	30710
9.02	4.813	87.22	154.1	192.29	242.2	283.89	33920
9.60	5.723	88.47	155.8	194.63	244.6	283.91	38400
10.29	6.907	89.72	157.4	196.96	246.9	283.93	42780
11.00	8.228	90.98	158.7	199.28	249.2	283.96	35050
11.69	9.659	92.24	160.0	201.60	251.6	284.01	57340
12.39	11.08	93.51	161.2	203.91	254.3	284.04	88270
13.55	13.66	94.79	162.3	206.20	258.5	284.07	128400
14.81	16.72	96.08	163.4	208.47	268.3	284.10	186000
16.03	19.84	97.37	164.4	210.73	262.6	284.14	170600
17.15	22.84	98.67	165.5	212.57	266.1	285.10	5219
18.21	25.76	99.98	166.5	213.98	270.9	286.42	634.8
19.21	28.60	101.29	167.6	215.37	278.4	287.82	635.8
20.21	31.44	102.61	168.6	216.74	293.6	289.91	637.3
21.21	34.25	103.93	169.7	218.10	287.1	292.02	638.6
22.20	37.05	105.26	170.7	219.51	271.3	294.14	639.9
23.20	39.89	106.60	171.7	220.95	272.9	296.29	641.0
24.23	42.72	107.95	172.7	222.40	274.5	298.47	642.1
25.29	45.62	109.30	173.8	223.85	276.2		
26.42	48.64	110.66	174.9	225.31	277.9	annealed	
27.62	51.81	112.02	175.9	226.77	279.6		
28.83	55.08	113.39	177.0	228.24	281.3	60.23	117.3
30.04	58.32	114.77	178.0	229.71	283.1	61.42	119.1
31.24	61.22	116.16	179.1	231.68	285.7	62.61	120.8
32.43	64.21	117.54	180.2	234.15	288.7	63.80	122.5
33.62	67.13	118.43	180.8	236.60	291.9	65.00	124.2
34.80	69.96	119.83	181.9	239.05	295.1	66.20	125.9
35.98	72.71	121.24	182.9	241.49	298.4	67.40	127.5
37.13	75.31	122.66	184.0	243.91	301.9	68.61	129.1
38.26	77.80	124.08	185.1	246.33	305.3	69.81	130.7
39.38	80.21	125.51	186.2	248.73	308.9	71.03	132.3
40.52	82.59	126.95	187.3	251.13	312.8	72.96	134.8
41.72	85.03	128.39	188.4	253.51	316.7	74.19	136.3
42.99	87.56	129.83	189.5	255.89	321.2	75.42	137.8
44.26	89.81	131.29	190.7	258.26	326.2	76.66	139.3
45.52	92.52	132.75	191.8	260.61	331.8	77.90	140.8
46.79	94.90	134.51	193.2	262.93	338.1	79.14	142.3
48.05	97.23	136.22	194.6	265.23	345.6	80.38	143.9
49.37	99.64	137.93	196.0	267.26	353.8	81.62	145.5
50.73	102.1	139.64	197.5	268.81	361.0	82.86	147.2
52.09	104.4	141.36	199.0	270.13	369.0	84.11	148.8
53.46	106.7	143.08	200.6	271.43	378.9	85.36	150.4
54.47	108.3	144.79	202.1	272.71	391.2	86.61	152.1
55.57	110.1	146.52	203.5	273.97	407.4	87.87	153.7
56.72	112.0	148.24	204.9	275.19	429.4	89.13	155.3

Table I. (continued)

T_{av}/K	$C_{p,m}$/J K^{-1} mol^{-1}	T_{av}/K	$C_{p,m}$/J K^{-1} mol^{-1}	T_{av}/K	$C_{p,m}$/J K^{-1} mol^{-1}	T_{av}/K	$C_{p,m}$/J K^{-1} mol^{-1}
57.89	113.8	149.97	206.2	276.36	460.0	90.39	156.9
59.08	115.6	151.70	207.6	277.48	504.2	91.67	158.4
60.27	117.4	153.44	209.0	278.51	567.9	92.94	159.8
61.46	119.2	155.18	210.5	279.44	661.6	94.23	161.1
62.65	121.0	156.92	211.9	280.26	798.4	95.52	162.4
63.84	122.6	158.67	213.6	280.95	996.1	96.81	163.6
65.04	124.3	160.41	216.3	281.52	1274	98.11	164.8
66.24	126.0	162.17	216.0	281.97	1651	99.42	165.9
67.44	127.6	163.93	217.5	282.34	2142	100.74	166.9
68.65	129.2	165.69	219.0	282.62	2764	102.06	168.0
69.86	130.7	167.46	220.4	282.85	3465	103.39	169.1
71.07	132.3	169.23	221.9	283.04	4343	104.73	170.2
72.29	133.8	171.00	223.4	283.19	5436	106.07	171.2
73.52	135.4	172.73	224.6	283.31	6649	107.42	172.3
74.76	136.8	174.47	226.2	283.41	8021	108.77	173.3
76.00	138.3	176.20	227.8	283.49	9600		
77.24	139.8	177.95	229.3	283.57	11340		
78.49	141.4	179.69	230.8	283.63	13290		

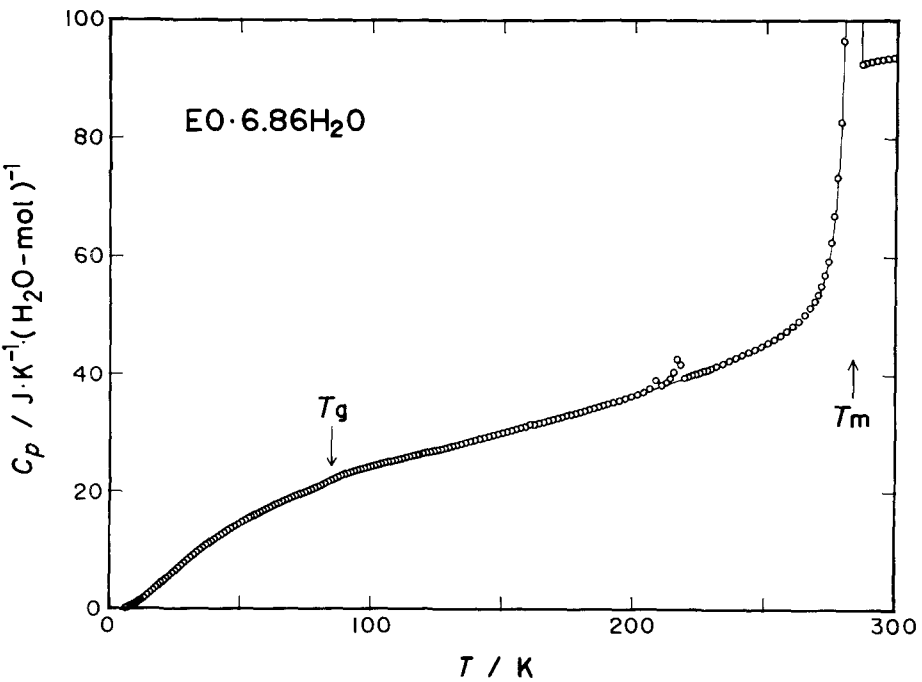

Fig. 1. Heat capacity of EO·6.86 H_2O. T_g and T_m represent the glass transition and the congruent melting temperatures, respectively.

As reported above, EO reacts with water to give ethylene glycol and diethylene glycol and so it is conceivable that small amounts of the two glycols were present in the starting material as the calorimeter cell was left at room temperature for half a day before being cooled down for the heat capacity measurements. The anomalies at 208 K and 217 K can tentatively be assigned to the eutectic meltings of the glycols and ice (or their hydrates).

The excess enthalpies of the anomalies at 160, 208, and 217 K correspond, respectively to 0.01%, 0.10%, and 0.26% of the enthalpy of congruent melting of EO-hydrate. The amounts of the impurities are very small and their effect on the heat capacity of EO·6.86 H_2O should be well within the accuracy of the calorimeter (0.2–0.3%). Therefore these anomalies will be neglected in the following analysis of the heat capacity results.

3.2. CONGRUENT MELTING AND STANDARD THERMODYNAMIC FUNCTIONS

As seen in Figure 1, the sample contained no ice, as indicated by the absence of the ice eutectic at 271 K [27]. The congruent melting temperature of EO·6.86 H_2O was determined to be (284.11 ± 0.02) K and is in good agreement with the value of 284.2 K for EO·6.89 H_2O reported by Glew and Rath [24]. Other values reported in the literature are (283.2 ± 0.4) K for EO·6.89 H_2O by Leaist *et al.* [20] and 284.6 K for a hydrate of unspecified composition by Callanan and Sloan [21]. The baseline for the melting anomaly was established by extrapolating the heat capacity data in the ranges 230–255 K and 286–298 K to 284.11 K. The enthalpy of congruent melting was determined to be 48.26 kJ mol^{-1} and compares well with the value (48 ± 1) kJ mol^{-1} reported by Leaist *et al.* [20] but is 2.4% lower than the value of 49.4 kJ mol^{-1} reported by Callanan and Sloan [21].

The heat capacity difference between the aqueous solution and the hydrate at 284.11 K was determined to be 279.2 JK^{-1} mol^{-1}; this gives the enthalpy of melting at 273.15 K as 45.20 kJ mol^{-1}. The error due to the uncertainty of the baseline including the effect of vaporisation of the solution was estimated to be less than 5 J mol^{-1}.

Standard thermodynamic functions were derived from the heat capacity results and are given in Table II as the quantities per mole of EO·6.86 H_2O. The values below 6 K were calculated from the extrapolation function:

$$C_p/(\mathrm{JK^{-1}\,mol^{-1}}) = a(T/\mathrm{K})^3 + b(T/\mathrm{K})^5 + c(T/\mathrm{K})^7. \quad (1)$$

The coefficients for Equation (1) were determined by fitting the heat capacity results between 6 and 15 K; the values are $a = 7.239 \times 10^{-3}$, $b = -8.062 \times 10^{-6}$, $c = -7.013 \times 10^{-9}$. There are two standard heat capacity values for 90 K in Table II. This arises from the fact that the heat capacity jump due to the glass transition occurs at 90 K.

3.3. GLASS TRANSITION

Figure 2 shows plots of encraty (C_p/T) (upper) and of spontaneous temperature drift rates, observed 15 min after each heating, against temperature. Open circles and triangles represent the results of the rapidly cooled and the annealed samples,

Table II. Standard thermodynamic functions of EO·6.86 H_2O

T / K	$C^0_{p,m}/R$	$[H^0_m(T) - H^0_m(0)]/RT$	$[S^0_m(T) - S^0_m(0)]/R$	$-[G^0_m(T) - H^0_m(0)]/RT$
5	(0.10)[a]	(0.0267)[a]	(0.0357)[a]	(0.0089)[a]
10	0.765	0.2005	0.2697	0.0692
15	2.066	0.5931	0.8109	0.2177
20	3.708	1.163	1.626	0.4629
30	6.986	2.567	3.761	1.193
40	9.803	4.037	6.171	2.134
50	12.12	5.427	8.613	3.186
60	14.08	6.710	11.00	4.291
70	15.74	7.885	13.30	5.414
80	17.19	8.960	15.50	6.539
90	18.48[b]	9.947	17.60	7.652
90	19.05[b]	9.947	17.60	7.652
100	20.04	10.91	19.66	8.750
110	20.97	11.78	21.61	9.831
120	21.88	12.58	23.47	10.89
130	22.83	13.33	25.26	11.93
140	23.81	14.05	26.99	12.94
150	24.79	14.73	28.67	13.94
160	25.78	15.39	30.30	14.91
170	26.77	16.03	31.89	15.86
180	27.79	16.66	33.45	16.79
190	28.88	17.27	34.98	17.71
200	30.05	17.88	36.49	18.61
210	31.32	18.49	37.99	19.50
220	32.68	19.10	39.48	20.37
230	34.11	19.72	40.96	21.24
240	35.64	20.35	42.44	22.09
250	37.40	21.00	43.93	22.93
260	39.72	21.67	45.44	23.77
270	44.29	22.41	47.01	24.60
273.15	47.66	22.68	47.54	24.86
280	90.85	23.59	49.02	25.43
290	76.64	44.41	71.10	26.69
298.15	77.24	45.30	73.23	27.93

[a] Quantities extrapolated from the data above 6 K (see text for details).
[b] Heat capacity jump due to the glass transition was assumed to occur at 90 K.

respectively. Exothermic drift followed by an endothermic drift appeared in the temperature range 65–95 K in the rapidly cooled sample and only a larger endothermic drift starting at the annealing temperature of 76.6 K appeared in the annealed sample. At first glance, these seem to be the temperature drift behavior typical of a glass transition [7, 8, 12, 14]. However, a comparison of the temperature drifts with the encraty results shows that the present glass transition is not a typical one. Usually, heat capacity shows a jump around the temperature (T_g) at which the sign of the temperature drift rates changes from a positive to a negative value. This is

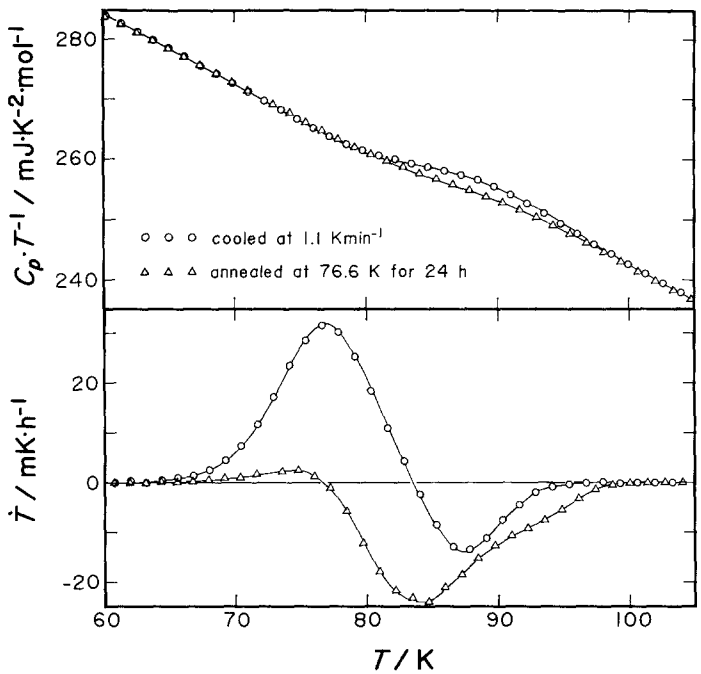

Fig. 2. Encraty (upper) and the corresponding temperature drift rate (lower) of EO·6.86 H_2O in the temperature range of the glass transition.

caused by the fact that the mode related to the glass transition contributes to the heat capacity at higher temperatures but not at a temperature lower than T_g. In the glass transitions observed previously, it was found that T_g was lower and the anomaly in the encraty plot larger for the annealed sample compared with the corresponding quantities for the rapidly cooled sample. However, in the present case we find that the behavior is just the opposite i.e. the anomaly in the encraty plot is smaller for the annealed sample and that this anomaly starts at a temperature higher than in the case of the rapidly cooled sample. Furthermore, the present glass transition is also unusual in the sense that the heat capacity jump is spread over a wide temperature range.

The most plausible explanation for the unusual behavior is that there is a wide distribution of the relaxation time in the system governing the glass transition and that the relaxation time becomes longer by annealing. Taking into consideration the fact that the glass transition in THF-hydrate is almost normal, though a small distribution of the relaxation time is observed, the anomalies in EO-hydrate are considered to be related to the following characteristic features of EO-hydrate: (1) It belongs to the structure I type containing the 14-hedral cages which are the most asymmetric compared to all the other cage types in structures I and II. (2) EO occupies both the 12- and the 14-hedral cages in structure I (about 70% of the 12-hedra are empty) whereas THF occupies mostly the 16-hedra in structure II. (3) The EO molecules are enclathrated tightly in the cages, especially in the 12-hedral

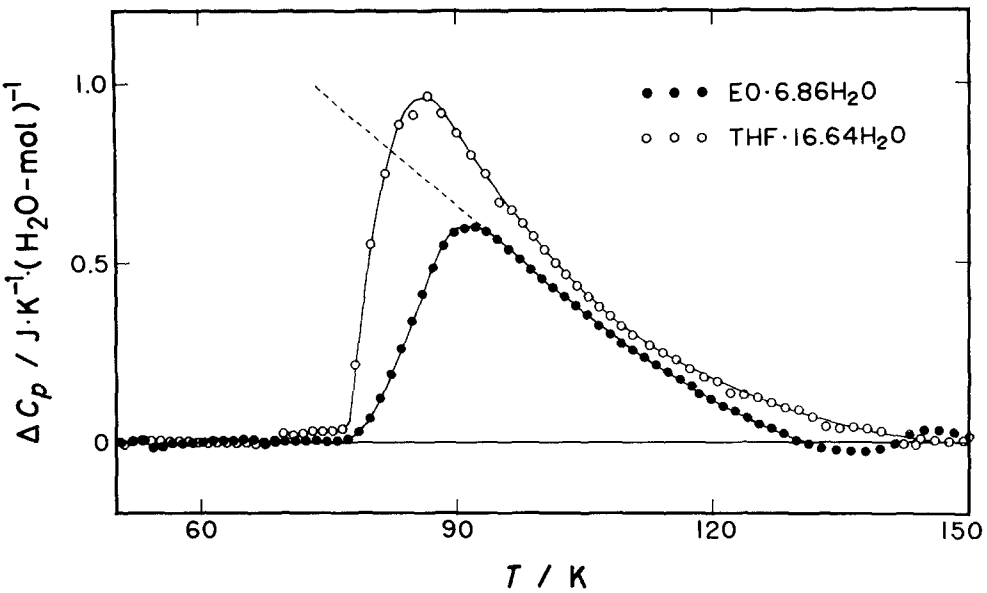

Fig. 3. Excess heat capacity of EO·6.86 H_2O (●) and THF·16.64 H_2O (○) in the temperature range of the glass transitions. Dashed line represents the hypothetical equilibrium heat capacity.

cages, and so the guest-host interaction is fairly strong compared with that in THF-hydrate.

Figure 3 shows the excess heat capacities in the glass transition regions of EO-hydrate (●) and THF-hydrate (○). For EO-hydrate, the baseline to be subtracted from the total heat capacity was determined by fitting the results in the ranges 40–75 K and 130–180 K with the fifth-order polynomials. The procedure is almost the same as that used for determining the baseline for THF-hydrate [12]. From studies of the neat and KOH-doped THF-hydrate, it was concluded that the excess heat capacity was due to the short-range ordering of protons in the hydrogen-bonded host lattice. Taking into consideration the fact that the T_g of EO-hydrate almost agrees with that expected from the dielectric results [18], the glass transition of EO-hydrate is also ascribed to freezing of the short-range ordering of protons in the host lattice. It is interesting to note that the excess heat capacities due to the short-range ordering of protons are almost the same, in shape and magnitude, in both hydrates in spite of the difference in the host structure, though the glass transition temperature of EO-hydrate is a little higher than that of THF-hydrate.

3.4. RELAXATION TIME ANALYSIS

In a system with a distribution of the relaxation time, it is difficult to analyze the enthalpy relaxation process of the glass transition in the manner usually performed for a system with a single relaxation time. In the low temperature region of the glass transition where the amount of relaxed enthalpy is small and the shape of the

distribution function does not change much with temperature, the relaxation time as a function of temperature gives information about the average activation enthalpy for the mode associated with the glass transition.

Figure 4 shows the configurational enthalpy related to the glass transition as a function of temperature. The step-like curve represents the actual path followed by the rapidly cooled sample in the heat capacity measurements. Each horizontal segment represents the temperature increase induced by electrical heating and each vertical segment the spontaneous exothermic enthalpy relaxation. Arrows represent the direction along which the heat capacity measurements were carried out. The smooth curve represents the equilibrium enthalpy derived from the hypothetical equilibrium heat capacity extrapolated to lower temperatures as shown by the dashed line in Figure 3. The zero of configurational enthalpy ΔH_c was taken at the temperature at which the temperature drift changed from a positive to a negative value.

The relaxation rate of the configurational enthalpy ($d\Delta H_c/dt$) is usually related to the relaxation time τ, when τ is single and time-independent, and ΔH_c is given by the equation [28]:

$$\frac{d\Delta H_c(T, t)}{dt} = -\frac{\Delta H_c(T, t)}{\tau(T)}. \tag{2}$$

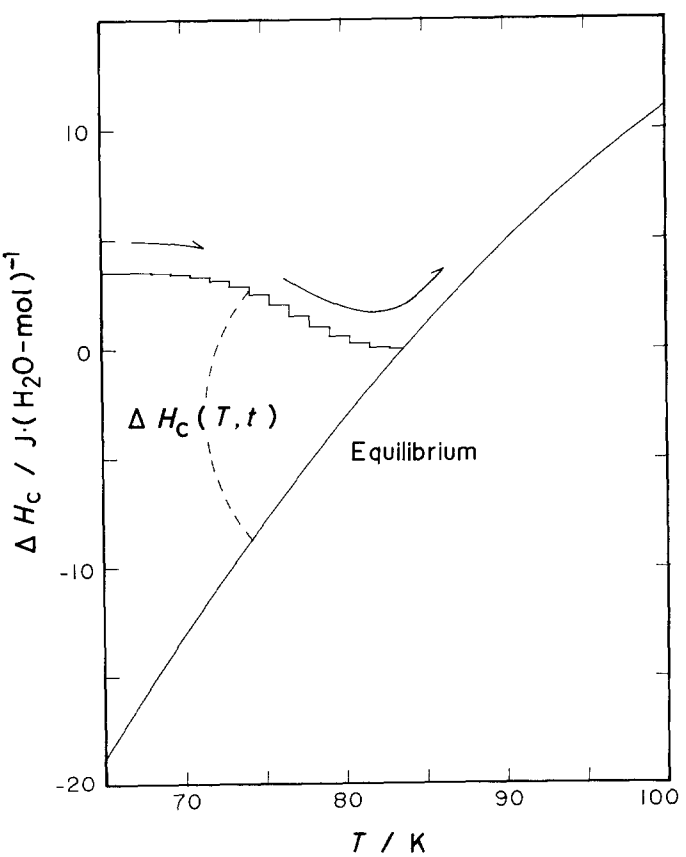

Fig. 4. Configurational enthalpy change due to the glass transition of EO·6.86 H_2O.

The rate of enthalpy relaxation at various temperatures ($d\Delta H_c/dt$) was obtained experimentally and ΔH_c, the enthalpy difference between the equilibrium and the non-equilibrium states at a given temperature, was obtained as shown in Figure 4. The relaxation times at temperatures lower than T_g were calculated from Equation (2) using the procedure described previously [12] and are shown by closed circles in Figure 5. Open circles in Figure 5 represent the relaxation times of THF-hydrate around its glass transition region [12].

As seen in Figure 5, the relaxation time becomes nonlinear with increasing temperature. This is most likely due to a distribution of the relaxation time. The lines in Figure 5 were obtained by fitting the relaxation times at lower temperatures (the lowest five points in case of EO-hydrate) to the Arrhenius equation:

$$\tau = A \exp(\Delta H_a/RT). \tag{3}$$

The slope of the line, ΔH_a, gives the activation enthalpy of the proton configurational motion. It was calculated to be 19.7 kJ mol^{-1} for EO-hydrate, for comparison the value for THF-hydrate is 19.4 kJ mol^{-1} [12]. Thus the activation enthalpies in EO and THF hydrates are almost the same and indicate that the mechanism responsible for excitation of the proton configurational motion in the two systems is quite similar. It appears that not only the static short-range ordering but also the dynamic activation mechanism for the proton configurational mode does not depend on the structure of the host.

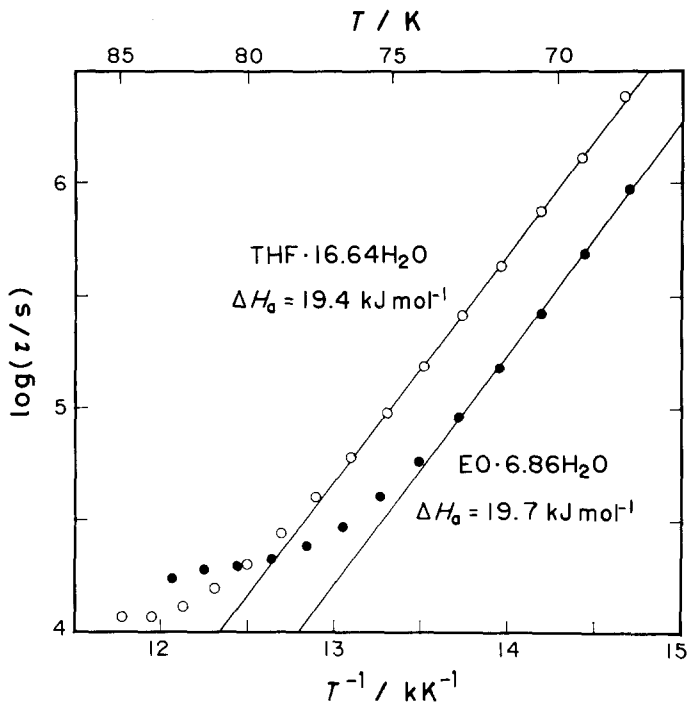

Fig. 5. Arrhenius plots of the enthalpy relaxation times of EO·6.86 H_2O (●) and THF·16.64 H_2O (○). The straight lines are representations of the low temperature data given by Equation (3).

3.5. ANALYSIS OF THE ENTHALPY RELAXATION WITH THE KOHLRAUSCH-WILLIAMS-WATTS FUNCTION

It is well known that relaxations in many condensed systems are characterised by a broad distribution of relaxation times and nonlinearity. The latter means that the time dependence of the relaxation process depends on the magnitude and sign of the perturbation that brings the material out of thermal equilibrium. Both these features are well described phenomenologically by the Kohlrausch-Williams-Watts (KWW) function [29, 30]. Many experimental observations for viscous liquids and glasses [31] can be reproduced by this function. It was recently observed that the relaxation in a crystal was not an exceptional case. Matsuo *et al.* [32] observed that the enthalpy relaxation in KCN-KBr mixed crystals actually showed non-exponential behavior. The enthalpy relaxation in this system was analysed using the following modified form of the KWW function [32]:

$$T(t) = A + Bt - C \exp[-(t/\tau)^{\beta}], \tag{4}$$

where $T(t)$ is the temperature at time t, $(A - C)$ the initial temperature, B the constant drift rate due to residual heat leak, C the amplitude of the relaxation, τ the relaxation time, and β the KWW parameter. The rate of enthalpy relaxation is proportional to the rate of the spontaneous temperature drift because of constancy of the heat capacity within the small temperature change (0.2 K) induced by the enthalpy relaxation (see Figure 6).

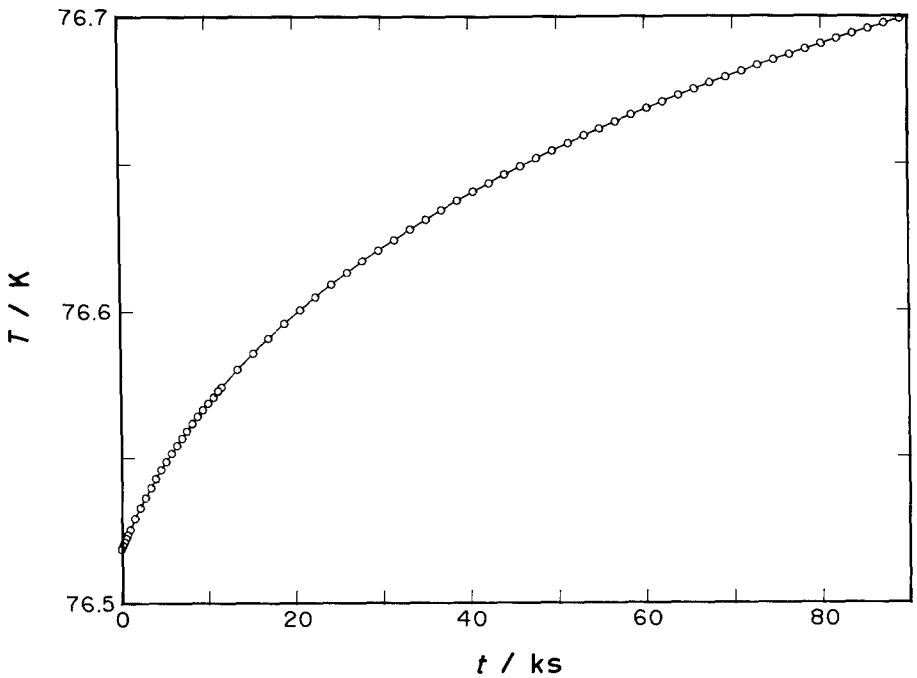

Fig. 6. Typical exothermic temperature drift due to the glass transition of EO·6.86 H_2O observed in the rapidly cooled sample at 76 K. The line represents the fit of the data given by Equation (4).

The KWW function, originally proposed as an empirical equation to describe the non-exponential behavior of relaxation processes, can be derived from several models which attach different physical meaning to β. Lindsey and Patterson [33] interpreted β as the extent of distribution of the relaxation time. The smaller β is, the broader the distribution function becomes. For $\beta = 1$, corresponding to a single relaxation time, the KWW function becomes the same as that derived by integrating Equation (2). In view of the distribution of the relaxation time among the hydrate cages described above (Section 3.4), we have analysed the enthalpy relaxation of EO-hydrate using Equation (4).

A number of experiments were conducted where the EO-hydrate was successively cooled at the rate of 2–3 K min^{-1} from 120 K to about 76, 80, 84, 88, and 92 K and exothermic temperature drifts observed for 3–25 h. The data at each temperature were fitted by the method of least-squares to Equation (4); the fits at all temperatures were quite satisfactory. Figure 6 shows a typical example of the temperature drift observed at ~76 K and the fitted curve. Values of the parameter β obtained were as follows:

T/K	76	80	84	88	92
β	0.41	0.45	0.54	0.43	0.40

At all temperatures except 84 K, the value of β ranges between 0.4 and 0.45 indicating that the distribution of relaxation time is quite wide and almost temperature independent. The result is consistent with the conclusion derived in section 3.3. from an analysis of the drift rates and the encraty shown in Figure 2.

The nature of the configurational disorder in the host lattice of EO-deuterohydrate at 80 K was studied by Hollander and Jeffrey [36] using neutron diffraction. The results gave no evidence of departure from the half-hydrogen model. This is in agreement with the present observation that the glass transition occurs at the very initial stage of development of short-range order of protons, as judged from the size of excess heat capacity. Prolongation of the relaxation time for the configurational change hinders the crystal from developing a long-range order on further cooling in the actual experiment.

In conclusion, the glass transitions in EO and THF hydrates are broadly similar. It would be of interest to study KOH-doped EO-hydrate to see if it also undergoes a first-order phase transition as found in the cases of ice I_h [10, 11] and THF-hydrate [12].

Acknowledgement

The authors thank Mr M. Bednas for providing gas chromatographic analyses. YPH thanks the National Research Council of Canada for leave to visit Osaka University. This work was supported partly by a Grant-in-Aid for Scientific Research No. 57430002 from the Ministry of Education, Science, and Culture, and partly by the Takeda Science Foundation.

References

1. J. E. Bertie and S. M. Jacobs: *Can. J. Chem.* **55**, 1777 (1977).
2. J. E. Bertie and S. M. Jacobs: *J. Chem. Phys.* **69**, 4105 (1978).

3. D. D. Klug and E. Whalley: *Can. J. Chem.* **51**, 4062 (1973).
4. G. P. Johari and H. A. M. Chew: *Phil. Mag. B* **49**, 281 (1984).
5. A. W. Naumann and G. J. Safford: *J. Chem Phys.* **47**, 867 (1967).
6. D. W. Davidson: in *Natural Gas Hydrates: Properties, Occurrence and Recovery*, Ed. J. L. Cox, Ch. 1, Butterworth, Boston (1983).
7. O. Haida, T. Matsuo, H. Suga, and S. Seki: *J. Chem. Thermodyn.* **6**, 815 (1974).
8. O. Yamamuro, M. Oguni, T. Matsuo, and H. Suga: *J. Phys. Chem. Solids* **48**, 935 (1987).
9. Y. P. Handa, D. D. Klug, and E. Whalley: *J. Phys. Colloq. C*1 **48**, 435 (1987).
10. Y. Tajima, T. Matsuo, and H. Suga: *Nature* **299**, 810 (1982).
11. Y. Tajima, T. Matsuo, and H. Suga: *J. Phys. Chem. Solids* **45**, 1135 (1984).
12. O. Yamamuro, M. Oguni, T. Matsuo, and H. Suga: *J. Phys. Chem. Solids* **49**, 425 (1988).
13. O. Yamamuro, M. Oguni, T. Matsuo, and H. Suga: *Solid State Commun.* **62**, 289 (1987).
14. O. Yamamuro, M. Oguni, T. Matsuo, and H. Suga: *J. Incl. Phenom.* **6**, 307 (1988).
15. M. von Stackelberg and B. Meuthen: *Z. Electrochem.* **62**, 130 (1958).
16. R. K. McMullan and G. A. Jeffrey: *J. Chem. Phys.* **42**, 2725 (1965).
17. D. W. Davidson and G. J. Wilson: *Can. J. Chem.* **41**, 1424 (1963).
18. S. K. Garg, B. Morris, and D. W. Davidson: *J. Chem. Soc., Faraday Trans. 2* **68**, 481 (1972).
19. J. E. Bertie and D. A. Othen: *Can. J. Chem.* **50**, 3443 (1972).
20. D. G. Leaist, J. J. Murray, M. L. Post, and D. W. Davidson: *J. Phys. Chem.* **86**, 4175 (1982).
21. J. E. Callanan and E. D. Sloan: *Int. Gas Res. Conf.* 1012 (1983).
22. O. Yamamuro, M. Oguni, T. Matsuo, and H. Suga: *Bull. Chem. Soc. Jpn.* **60**, 1269 (1987).
23. O. Maass and E. H. Boomer: *J. Am. Chem. Soc.* **44**, 1709 (1922).
24. D. N. Glew and N. S. Rath: *J. Chem. Phys.* **44**, 1710 (1966).
25. K. E. MacCormack and J. H. B. Chenier: *Ind. Eng. Chem.* **47**, 1454 (1955).
26. W. F. Giauque and J. Gordon: *J. Am. Chem. Soc.* **71**, 2176 (1949).
27. D. N. Glew and M. L. Haggett: *Can. J. Chem.* **46**, 3857 (1968).
28. H. Suga and S. Seki: *J. Non-Cryst. Solids* **16**, 171 (1974).
29. R. Kohlrausch: *Ann. Phys. (Leipzig)* **12**, 393 (1847).
30. G. Williams and D. C. Watts: *Trans. Faraday Soc.* **66**, 80 (1970).
31. S. Brawer: in *Relaxation in Viscous Liquids and Glasses*, American Ceramic Society, Columbus, Ohio (1985).
32. T. Matsuo, I. Kishimoto, H. Suga, and F. Luty: *Solid State Commun.* **58**, 177 (1986).
33. C. P. Lindsey and G. D. Patterson: *J. Chem. Phys.* **73**, 3348 (1980).
34. R. G. Palmer, D. L. Stein, E. Abrahams, and P. W. Anderson: *Phys. Rev. Lett.* **53**, 958 (1984).
35. K. L. Ngai, R. W. Rendell, A. K. Rajagopal, and S. Teitler: *Ann. N. Y. Acad. Sci.* **484**, 150 (1986).
36. F. Hollander and G. A. Jeffrey: *J. Chem. Phys.* **66**, 4699 (1977).